Biosensors and Bioelectronics 30 (2011) 333–336

Contents lists available at SciVerse ScienceDirect

Biosensors and Bioelectronics

journal homepage: www.elsevier.com/locate/bios

Short communication

Highly sensitive and selective uric acid biosensor based on RF sputtered NiO thin film

Kashima Arora[a], Monika Tomar[b], Vinay Gupta[a,*]

[a] Department of Physics and Astrophysics, University of Delhi, Delhi 110007, India
[b] Physics Department, Miranda House, University of Delhi, Delhi 110007, India

ARTICLE INFO

Article history:
Received 22 July 2011
Received in revised form
17 September 2011
Accepted 20 September 2011
Available online 29 September 2011

Keywords:
Thin films
Sputtering
NiO
Uric acid
Biosensor

ABSTRACT

Present study highlights the importance of RF sputtered NiO thin film deposited on platinum coated glass substrate (NiO/Pt/Ti/glass) as a potential matrix for the realization of highly sensitive and selective uric acid biosensor. Uricase has been immobilized successfully onto the surface of NiO matrix by physical adsorption technique. The prepared bioelectrode (uricase/NiO/Pt/Ti/glass) is utilized for sensing uric acid using the cyclic voltammetry and UV visible spectroscopy techniques. The bioelectrode is found to exhibit highly efficient sensing response characteristics with high sensitivity of 1278.48 μA/mM; good linearity of 0.05–1.0 mM, and very low Michaelis–Menten constant (k_m) of 0.17 mM indicating high affinity of uricase towards the analyte. The enhanced response is due to the development of NiO matrix with good electron transport property and nanoporous morphology for effective loading of enzyme with preferred orientation.

1. Introduction

Rapid growth in the development of new materials and improvements in sensing techniques have led to the evolution of advanced biosensors which have potential application in the field of healthcare, biological analysis, environment monitoring and food industries. Uric acid is an end product of purine metabolism in human body, a number of diseases and pathological disorders are related to its high concentration in body fluids (e.g. serum and urine), such as gout, arthritis, kidney disease, cardiovascular disease, and neurological diseases. Consequently, uric acid determination is of paramount importance in the diagnosis of the diseases caused by disorder of purine biosynthesis and catabolism. Various matrices including metal nanoparticles, conducting polymer, metal oxide thin films, etc. have been exploited to immobilize uricase to fabricate uric acid biosensor. Amongst them, ZnO based metal oxide matrices have attracted considerable interest of the research community due to their high reproducibility, stability and shelf life. However, ZnO is known to have intrinsic native defects related to zinc and oxygen, which hinders its charge transfer characteristics giving limited sensitivity.

Hence, there is an urgent need to identify an alternate matrix, which gives stable and enhanced biosensing response characteristics especially for uric acid. Recently, few reports have shown the importance of NiO thin film matrix for the realization of an integrated biosensor due to its good electrochemical behavior, oxygen ion conductivity, biocompatibility and high isoelectric point (IEP) ~ 10.7 (Li et al., 2008; Salimi et al., 2007; Zang et al., 2010; Safavi et al., 2009; Sattarahmady et al., 2010). Most of the biosensors are based on sol gel derived NiO thin films, however the electron transfer property of NiO was lower. Therefore, NiO/Chitosan composite matrix has been utilized for cholesterol biosensor. The polymer matrix, chitosan, has been incorporated with NiO to improve the electrical conductivity but it hampers the stability of the bioelectrode. The electron transfer property may depend on the growth kinetics of NiO thin film, and no efforts have been made towards the development of NiO thin films using reproducible RF sputtering technique for biosensing application despite the fact that it results in good quality metal oxide thin film with desired morphology and controlled stoichiometry. Furthermore, there is no report on the detection of uric acid based on NiO thin film matrix. Hence, in the present work good quality NiO thin films exhibiting good electron transfer property has been deposited by RF sputtering technique for the detection of uric acid. Uricase is successfully immobilized on the surface of NiO matrix by physical adsorption process and enhanced biosensing response characteristics of the prepared bioelectrode for uric acid have been determined. Uricase

* Corresponding author. Tel.: +91 09811563101.
E-mail address: vgupta@physics.du.ac.in (V. Gupta).

0956-5663/$ – see front matter © 2011 Elsevier B.V. All rights reserved.
doi:10.1016/j.bios.2011.09.026

catalyzes the in vivo oxidation of uric acid in the presence of oxygen to produce allantoin and CO_2 as oxidation products of uric acid and hydrogen peroxide as a reduction product of O_2. The uricase catalytic reaction is as follows:

$$\text{Uric acid} + H_2O + O_2 \xrightarrow{\text{Uricase}} \text{Allantoin} + CO_2 + H_2O_2$$

Formation of hydrogen peroxide is detected by the amperometric current measurement during oxidation at the electrode:

$$H_2O_2 \rightarrow O_2 + 2H^+ + 2e^-$$

The enzymatic electrochemical biosensor relies on shuttling of these electrons, generated in the biochemical reaction shown above, from the redox center of the enzyme to the electrode via NiO thin film matrix. Enzymes, because of their insulated-shell redox centers, are unable to show direct electrochemistry. The presence of a redox species (mediator $[Fe(CN)_6]^{3-/4-}$), in the system, provides the path for electron transfer from the redox centers of the enzyme to the electrode using good electron communication property of the prepared NiO matrix, which results in increase in peak oxidation and reduction currents. The current further increases linearly with the increase in the concentration of analyte (uric acid) in the solution.

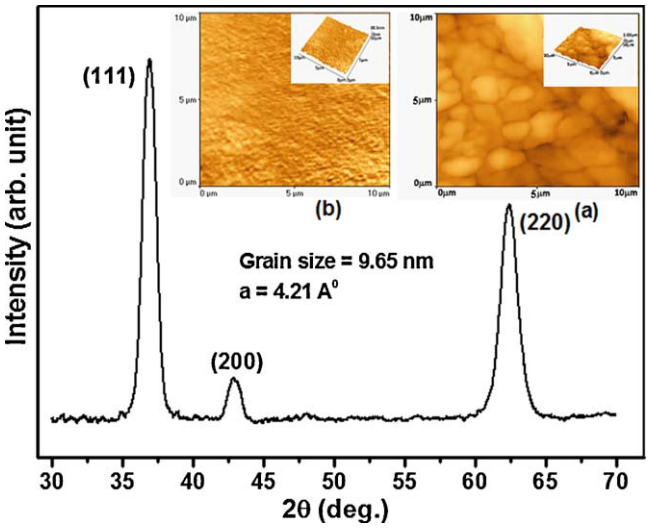

Fig. 1. XRD of NiO/Pt/Ti/glass electrode deposited at a substrate temperature of 400 °C. Inset shows AFM of (a) uricase/NiO/Pt/Ti/glass bioelectrode and (b) NiO/Pt/Ti/glass electrode.

2. Experimental

The schematic of bioelectrode prepared in the present study is shown in Supplementary Fig. 1. A 200 nm thin platinum (Pt) film was coated on corning glass substrate by RF sputtering technique using a Pt (99.99% pure) target in 100% Ar gas ambient at 10 mTorr sputtering pressure. The films were coated at room temperature substrate with an RF power of 100 W. The adhesion of Pt on corning glass substrate was found to be poor and therefore a thin buffer layer of Ti (~20 nm) was deposited prior to Pt thus yielding Pt/Ti/glass substrate. Nickel oxide (NiO) thin film matrix was deposited on the surface of Pt/Ti coated glass substrate (NiO/Pt/Ti/glass electrode) using a 2 in. diameter metallic nickel (Ni) target (99.99% pure) by RF sputtering technique using the optimized deposition conditions listed in Supplementary table I in different batches (four times). The NiO thin film was found to be transparent and strongly adherent to the substrate. The biolectrode (uricase/NiO/Pt/Ti/glass) was prepared by successfully immobilizing 10 μL of uricase (1.0 mg/mL, in 50 mM phosphate buffer of pH 7.0) on the surface of NiO thin film via physical adsorption technique. The prepared bioelectrode (uricase/NiO/Pt/Ti/glass) is kept overnight for drying at 4 °C.

X-ray diffraction (XRD) [Bruker D8 Discover] was used to identify the crystallographic structure of the deposited NiO thin film. Activity of the enzyme immobilized on the surface of NiO/Pt/Ti/glass electrode was studied by photometric assay using UV–vis spectrophotometer [PerkinElmer lamda 35]. Atomic force microscopy (AFM) [Veeco DICP2] was employed to study the surface morphology of the thin films. Cyclic voltammetric (CV) measurements were carried out on a potentiostat/galvanostat [Gamry Inc. 600] using a three-electrode system in PBS solution (50 mM, pH 7.0, 0.9% NaCl) containing a mediator of 5 mM $[Fe(CN)_6]^{3-/4-}$ with Ag/AgCl as the reference electrode.

3. Results and discussion

3.1. Structural and morphological studies

The as grown NiO thin film is found to be polycrystalline (Fig. 1) with pure cubic phase as indicated by a preferred oriented sharp XRD peak corresponding to (1 1 1) plane along with other diffraction peaks related to weak (2 0 0) and (2 2 0) planes. The lattice parameter (a = 4.21 Å) is found to be slightly higher than the corresponding bulk value (4.17 Å), which may be associated with the expanded lattice due to defects and give rise to tensile stress in the film. The crystallite size is calculated using the Debye–Scherrer formula (Cullity, 1978) using the preferred oriented (1 1 1) peak and is found to be about 10 nm.

AFM images of the surface of NiO thin film and uricase immobilized NiO surfaces are shown in the insets (b and a) of Fig. 1 respectively. The surface microstructure of NiO thin film shows uniformly distributed grains along with nanoporous morphology [Fig. 1 inset (b)]. The nanoporous structure provides larger surface area, which is advantageous for enhanced enzyme loading on the film surface. Roughness of the film surface (average root mean square roughness), an important parameter for sensing applications that plays a major role in the charge transfer capacity (Avellaneda et al., 2008) calculated using SPM Lab Analysis software, is about 3.7 nm. The same roughness has been obtained using a Dektak surface profiler (Dektak 150) as well. AFM micrograph of the surface of uricase/NiO/Pt/Ti/glass bio-electrode [Fig. 1 inset (a)] shows significant changes in the morphology. The uniformly distributed globular structure along with an increase in its average rms roughness from 3.7 to 30 nm was observed indicating the successful immobilization of uricase on the surface of NiO thin film matrix.

Supplementary Fig. 2 shows the FTIR spectra of uricase/NiO/Pt/Ti/glass bioelectrode. The FTIR spectra of NiO/Pt/Ti/glass electrode is also included in the inset for comparison. The bands at 684.1 and 461.7 cm^{-1} (inset (a) of Supplementary Fig. 2) correspond to the stretching vibration mode and the torsional vibration mode of Ni–O at the tetrahedral and octahedral sites respectively. The band at 578 cm^{-1} corresponds to the stretching of Ni–O–Ni in the nanoporous electrode, confirming the formation of NiO matrix and the absorption band at about 1632 cm^{-1} corresponds to H–O–H bending vibrations mode due to adsorption of water from atmosphere. The appearance of additional absorption bands at 1567.6 and 1652.5 cm^{-1} in FTIR spectra of uricase/NiO/Pt/Ti/glass bioelectrode (Supplementary Fig. 2) correspond to the primary and secondary amide linkages of enzyme molecule (uricase) indicating the immobilization of uricase on the surface of NiO thin film, which is in accordance with that of free uricase (inset (b) of Supplementary Fig. 2).

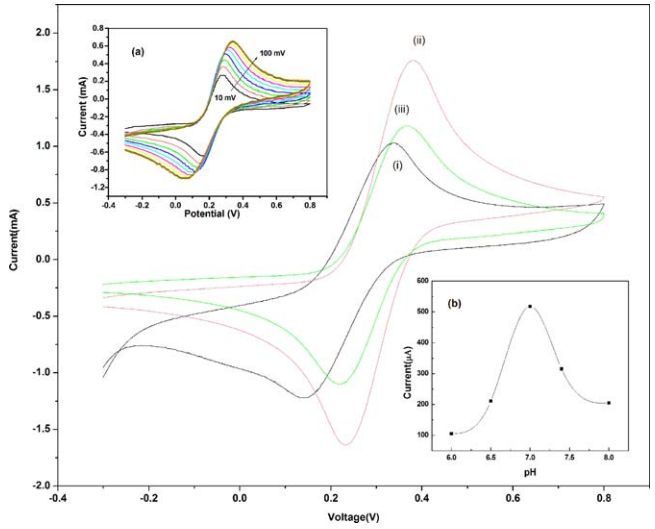

Fig. 2. CV of (i) Pt/Ti/glass, (ii) NiO/Pt/Ti/glass electrode and (iii) uricase/NiO/Pt/Ti/glass bioelectrode and insets show (a) CV of uricase/NiO/Pt/Ti/glass bioelectrode with scan rate and (b) effect of pH on the current response of uricase/NiO/Pt/Ti/glass bioelectrode.

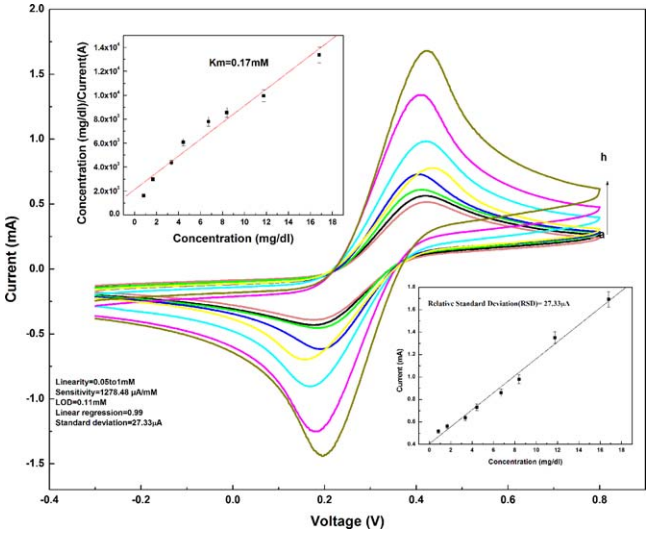

Fig. 3. Electrochemical response of uricase/NiO/Pt/Ti/glass bioelectrode as a function of uric acid concentration: (i) 0.05 (ii) 0.1 (iii) 0.2 (iv) 0.3 (v) 0.4 (vi) 0.5 (vii) 0.7 and (viii) 1.0 mM. Inset (a) variation of peak oxidation current as a function of concentration (b) Hanes plot to determine Michaelis–Menten constant (k_m).

3.2. Amperometric and photometric studies

Fig. 2 shows the CV curves obtained for the Pt/Ti/glass, NiO/Pt/Ti/glass and uricase/NiO/Pt/Ti/glass electrodes at a scan rate of 200 mV/s. It can be observed that the peak oxidation current for the NiO/Pt/Ti/glass electrode (1.77 mA) is more in comparison to that of Pt/Ti/glass electrode (1.02 mA) and is attributed to the enhanced electron transport property of deposited NiO matrix. Furthermore the effective loading of immobilized uricase on the nanoporous surface of the NiO film provides the increased electrocatalytic surface activity. The oxidation current decreases to 1.18 mA on immobilization of uricase onto the matrix surface (uricase/NiO/Pt/Ti/glass), which may be attributed to the non-conducting nature of enzyme (uricase). The immobilization of non-conducting enzyme on the surface of NiO/Pt/Ti/Glass electrode should results in an increase in a peak-to-peak separation of the redox peaks. However, an insignificant increase (~0.02 V) in the peak-to-peak separation was observed in the present work. This may be attributed to the occurrence of oxidation or reduction process at a relatively lower potential due to effective loading of immobilized uricase with preferred orientation on the nanoporous surface of NiO matrix. Therefore, even though some potential drop may occur across the bioelectrode due to presence of insulating enzyme, the observed increase in peak-to-peak separation is not significant. Inset (a) in Fig. 2 shows that maximum oxidation current for the uricase/NiO/Pt/Ti/glass bioelectrode is observed at a pH of 7.0 hence the pH of buffer is maintained at 7.0 for all the measurements.

The CV studies have been carried out on uricase/NiO/Pt/Ti/glass bioelectrode as a function of scan rate (ν) from 10 to 150 mV/s to determine the concentration of ionic species on its surface (inset (a) of Fig. 2). The oxidation peak was found to shift slowly towards higher potential and the reduction peak towards lower potential, with increase in scan-rate upto 80 mV/s suggesting a quasi-reversible process (Manesh et al., 2011). Since saturation (i.e. no more rise and shift in peak oxidation/reduction current and potential, respectively) is obtained at a scan rate of 90 mV/s as shown in inset (b) of Fig. 2, the range of scan rate for this study is taken from 10 to 80 mV/s. The linear regression equations for both the peak anodic as well as cathodic currents are given as:

$$I_{pa} = 0.066\nu^{1/2} + 0.088 \quad \text{with} \quad R = 0.99 \quad \text{and} \quad SD = 0.015 \qquad (1)$$

$$I_{pc} = -0.044\nu^{1/2} - 0.127 \quad \text{with} \quad R = -0.99 \quad \text{and} \quad SD = 0.014 \qquad (2)$$

where R is regression coefficient and SD is the standard deviation. Value of R close to 1 and $SD \ll 1$ indicate that both the anodic (I_{pa}) and cathodic (I_{pc}) peak currents increase linearly with the square root of scan rate ($\nu^{1/2}$), suggesting that the electrode reaction is a diffusion assisted electron-transfer process (Yang et al., 2006). The plot of anodic peak potential (E_{pa}) with logarithm of scan rate (ν) was linear. Surface concentration (Γ) of the ionic species per unit surface area of uricase/NiO/Pt/Ti/glass bioelectrode is estimated using the Brown–Anson model (Kaushik et al., 2008) based on the following equation:

$$I_{pa} = \frac{n^2F^Z\Gamma A\nu}{4RT},$$

where Γ is the estimated value of surface coverage in mol cm^{-2}; I_{pa}/ν can be calculated from the slope of I_{pa} vs. ν plot, and found to be 2.3×10^{-7} mol cm^{-2} which is relatively higher (Yogeswaran and Chen, 2007). The results show that the RF sputtered NiO thin film matrix is providing better platform for the immobilization of the receptor biomolecules.

Electrochemical response studies of uricase/NiO/Pt/Ti/glass bioelectrode as a function of uric acid concentration at a scan rate of 50 mV/s are shown in Fig. 3. The results show that the current response increases linearly with increasing uric acid concentration (inset (a) of Fig. 3) in the range 0.05–1 mM (0.15–0.45 mM physiological range), which is much higher as compared to the one reported on uric acid biosensor (Ahuja et al., 2010). The sensing response characteristics obtained with all prepared electrodes were found to be reproducible within ±2% accuracy over the entire range of uric acid, indicating the high repeatability of the prepared electrode.

The uricase/NiO/Pt/Ti/glass bioelectrode exhibits low response time of 5 s towards the analyte, which is much faster as compared to the reports available on metal oxide based uric acid biosensors by other workers (Syed et al., 2011). The prepared bioelectrode is highly reproducible (25 times) with a detection limit of about 0.11 mM (1.84 mg/dl), which is lower than the physiological

range. The lower detection limit is calculated using the expression $3s_{y/x}$/sensitivity, where $s_{y/x}$ is standard deviation obtained from the peak oxidation current vs analyte concentration curve (Matharu et al., 2009). Singh et al. (2011) utilized NiO nanostructures synthesized using chemical route for detection of cholesterol and reported a reproducibility of 11 times. The higher reproducibility (25 times) with enhanced sensitivity optimized in the present work highlights the importance of RF sputtered NiO thin film matrix for biosensing application.

The Michaelis–Menten constant (k_m) value of prepared bioelectrode is obtained using Hanes plot (inset (b) in Fig. 3) (Walker, 2000). The estimated value of k_m = 0.17 mM is obtained and is found to be much lower in comparison to the reported values (0.238 mM) for uric acid biosensor based on metal oxide matrices (Zhang et al., 2004). The low k_m value indicates that the bioelectrode based on RF sputtered NiO thin film has high affinity towards the uric acid which may be attributed to the alignment of immobilized uricase onto the NiO matrix is in favourable direction with higher loading.

Sensitivity of the prepared bioelectrode for uric acid is found to be 1278.48 μA/mM with linear regression coefficient of 0.99, which is much higher in comparison to the earlier reported results on uric acid biosensors based on other matices (Ahuja et al., 2010). The high sensitivity of the uricase/NiO/Pt/Ti/glass bioelectrode is attributed to the high electron transfer characteristics, excellent adsorption ability, high electrocatalytic activity and effective loading of enzyme on nanoporous surface of sputtered NiO thin film.

To carry out the photometric enzyme assay, the uricase/NiO/Pt/Ti/glass bioelectrode is dipped for 2 min in 3 mL PBS solution containing 20 μL horseradish peroxidise (HRP), 20 μL *o*-dianisidine dye and 100 μL of analyte (uric acid) in varying concentration. The difference between the initial and final absorbance of the prepared bio-electrode was measured at a fixed wavelength (500 nm) and their values were plotted as a function of uric acid concentration in Supplementary Fig. 3. The uricase enzyme activity increases with an increase in the concentration of uric acid (Supplementary Fig. 3). The amount of bound enzyme is determined from the apparent enzyme activity (a_{enz}^{app}) calculated using equation

$$a_{enz}^{app}(\mathrm{Ucm^{-2}}) = \frac{AV}{sts'}$$

where A is the difference in absorbance before and after incubation, V is the total volume (=3.17 cm^3), ε is the millimolar extinction coefficient for *o*-dianisidine (7.5 for *o*-dianisidine at 500 nm), t is the reaction time (2 min), and s is the surface area of the electrode (Saha et al., 2009). The value of apparent enzyme activity of uricase on the NiO/Pt/Ti/glass electrode is found to be about 4.14×10^{-2} unit/cm^2, indicating that 4.14×10^{-2} units of uricase are actively working on unit electrode surface area. The selectivity of uricase/NiO/Pt/Ti/glass bioelectrode is determined by measuring response current in CV analysis on addition of normal concentration of interferents in the human serum such as glucose (5.6 mM), cholesterol (5 mM), urea (1 mM), ascorbic acid (0.1 mM) and dopamine (0.1 mM) at normal concentration of uric acid (0.1 mM) indicating maximum interference of 2.5% (inset of Supplemenatry Fig. 3). The shelf life studies of the prepared uricase/NiO/Pt/Ti/glass bioelectrode shows that it retains more than 90% of activity even after 4 months which is much higher compared to the reports available on other biosensors based on NiO (Singh et al., 2011). This may be attributed to the highly stable and biocompatible NiO thin film matrix obtained in the present study using RF sputtering technique.

4. Conclusion

In conclusion, RF sputtered NiO thin film matrix with nanoporous morphology has been successfully exploited for uric acid biosensing in the physiological range due to its excellent electron transfer capabilities besides high adsorption ability and electrocatalytic activity. The uricase/NiO/Pt/Ti/glass bioelectrode exhibits high sensitivity of 1278.48 μA/mM, with fast response time of 5 s and low detection limit of 0.11 mM (lower than the lowest physiological range). The bioelectrode is reproducible atleast 24 times with a shelf life of about 4 months indicating that RF sputtered NiO thin film is an attractive matrix for realization of highly sensitive and stable uric acid biosensor.

Acknowledgements

Authors are thankful to University Grants Commission (UGC) and Department of Science and Technology (DST) for the financial support to carry out the proposed work. One of the authors (KA) is also thankful to the Council of Scientific and Industrial Research (CSIR), India for the research fellowship.

Appendix A. Supplementary data

Supplementary data associated with this article can be found, in the online version, at doi:10.1016/j.bios.2011.09.026.

References

Ahuja, T., Rajesh, Kumar, D., Tanwar, V.K., Sharma, V., Singh, N., 2010. Thin Solid Films 519, 1128.
Avellaneda, C.O., Berton, M.A.C., Bulhoes, L.O.S., 2008. Solar Energy Materials and Solar Cells 92, 240.
Cullity, B.D., 1978. Elements of X-Ray diffraction, 2nd ed. Reading, MA, Addison-Wesley, p. 102.
Kaushik, A., Solanki, P.R., Ansari, A.A., Ahmad, S., Malhotra, B.D., 2008. Electrochemistry Communications 10, 1364.
Li, C., Liu, Y., Li, L., Du, Z., Xu, S., Zhang, M., Yin, X., Wang, T., 2008. Talanta 77, 455.
Manesh, K.M., Kim, H.T., Santhosh, P., Gopalan, A.I., Lee, K.P., 2011. Journal of Electroanalytical Chemistry 654, 72.
Matharu, Z., Pandey, P., Pandey, M.K., Gupta, V., Malhotra, B.D., 2009. Electroanalysis 21, 1587.
Safavi, A., Maleki, N., Farjami, E., 2009. Biosensors and Bioelectronics 24, 1655.
Saha, S., Arya, S.K., Singh, S.P., Sreenivas, K., Malhotra, B.D., Gupta, V., 2009. Analytica Chimica Acta 653, 212.
Salimi, A., Sharifi, E., Noorbakhsh, A., Soltanian, S., 2007. Biophysical Chemistry 125, 540.
Sattarahmady, N., Heli, H., Faramarzi, F., 2010. Talanta 82, 1126.
Singh, J., Kalita, P., Singh, M.K., Malhotra, B.D., 2011. Applied Physics Letters 98, 123702.
Syed, M., Ali, U., Alvia, N.H., Ibupoto, Z., Nur, O., Willander, M., Danielsson, B., 2011. Sensors and Actuators B 152, 241.
Walker, J.M., 2000. Principles, Techniques of Practical Biochemistry, 5th ed. Cambridge University Press, UK.
Yang, M., Yang, Y., Yang, H., Shen, G., Yu, R., 2006. Biomaterials 27, 246.
Yogeswaran, U., Chen, S.M., 2007. Electrochimica Acta 52, 5985.
Zang, W.D., Jin, C., Chuan, J.L., Xiang, Y.Y., Qi, Z.J., 2010. Mikrochimica Acta 168, 259.
Zhang, F., Wang, X., Ai, S., Sun, Z., Wan, Q., 2004. Analytica Chimica Acta 519, 155.